Cement 10 (2022) 100050

Contents lists available at ScienceDirect

Cement

journal homepage: www.sciencedirect.com/journal/cement

Managing Thermal Effects in Waterproofed Concrete with Multi-Crystallization Enhancer

Radi Al-Rashed [a], Maher Al-Jabari [b,*]

[a] International Chem-Crete Corporation, 800 Security Row, Richardson, TX 75081 U.S.A
[b] Chem-Crete Europe, Stanicna 13, 90851, Holic, Slovakia

ARTICLE INFO

Keywords:
Concrete
Mass concrete
Hydration
Freezing and thawing
Permeability
Waterproofing
Crystallization
Hygroscopicity
Hydrophilicity
Hydrophobicity

ABSTRACT

Thermal effects in concrete are associated with a heat release from the exothermic cement hydration reactions during concrete curing under normal conditions or under severe cold conditions, or when it is subjected to cycles of freezing and thawing. These thermal effects may cause cracking, impact concrete porosity and affects its thermal, mass and hydraulic conductivities, and hence create major durability problems. This paper presets an experimental study of the thermal management ability of an aqueous waterproofing solution (the Multi-Crystallization Enhancer (MCE)) that is intermixed with water at the time of batching. The experiments were performed according to the applicable ASTM procedures for measuring the rate of heat release, temperature profiles, compressive and flexural strengths, temperature-time factor and thermal and electrical conductivities. Additionally, the impact of cycles of freezing and thawing on the percentages of mass change, length change and relative dynamic modulus were investigated. The findings indicate that the addition of the MCE at a dosage of 2% of cement weight has the potential to mitigate the thermal effects during cement hydration and during curing concrete under freezing conditions providing a solution for thermal problems of mass concrete. The findings demonstrate that the MCE can delay the exothermic heat release and can reduce its rate at the initial stage. It can also increase the resistance of concrete against cycles of freezing and thawing by achieving 92% reduction in the percentage mass change, 15% reduction in the percentage length change and 17% enhancement in the relative dynamic modulus, after 300 cycles. These thermal impacts of the MCE are also associated with 16% reduction in the thermal conductivity and 90.7% reduction in the total charge passage through concrete.

1. Introduction

Concrete structures are made of composite materials that involve networks of pores and voids, which facilitate the penetration of gasses and liquids and other transport processes, the theoretical aspects of which are detailed elsewhere [1]. When concrete is exposed to attacks associated with thermal, mechanical and chemical impacts, its durability declines and service life is shortened as a result of various physicochemical mechanisms [2]. Concrete durability can be defined the ability of concrete to resist any process of deterioration [3]. The durability is dependent on structure quality and watertightness which is governed by the concrete mix design and the type of additions [4]. In principle, a waterproofed and dense concrete with disconnected capillary networks can achieve long-time durability [5, 6]. Water interactions with cementitious surfaces include hydrophilicity (water swelling), hygroscopicity (vapor absorption), hydrophobicity (water-repelling) and icephobocity (ice detachment) as detailed elsewhere [7].

In this work, the focus is on concrete deterioration resulting from thermal transport processes associated with moisture interactions within pores. The thermal impacts are associated with the release of thermal energy (1) during the cement hydration process (for normal and mass concrete), (2) from casting concrete under severe cold conditions or (3) from subjecting the concrete to cycles of freezing and thawing. These problems are also affected by the concrete porosity and its thermal, mass and hydraulic conductivities. The theoretical aspects of these characteristics are based on the well-known equations of transport phenomena [1]. The physicochemical mechanisms of cement hydration process [8] include particle agglomeration, dissolution, diffusion, and reactions [9]. These mechanisms of cement hydration are associated with a release of a considerable amount of heat that raises the temperature of concrete within an initial time period of three days. The reaction of the main constituent in cement composition (C_3S) is five-times faster

* Corresponding author:
E-mail addresses: radi@chem-crete.com (R. Al-Rashed), mjabari@chem-crete.com, mjabari@ppu.edu (M. Al-Jabari).

https://doi.org/10.1016/j.cement.2022.100050
Received 29 March 2022; Received in revised form 29 August 2022; Accepted 16 November 2022
Available online 17 November 2022

than the second reacting constituent (C_2S) and it releases nearly double of the amount of heat [10]. The overall cement hydration reaction rate as a function of curing time can be determined by measuring the differential heat evolution curve from a typical cement hydration process [11–15]. The initial sources of heat release include the heat of solution (e.g. aluminates, and sulfates [13]), the heat of formation of ettringite. Then, the major part of heat liberation from the hydration of C_3S is released, within the first three days, which composes about 50% of the full heat release of the cement hydration. Increasing the temperature increases the rate of cement hydration [16]. The differential heat evolution curve is characterized by an initial slow constant rate of heat release (during the induction period of 2–5 h), resulting from the formation of a protective layer on the C_3S particles, followed by a major thermal peak. The heat release is accelerated gradually when such a protective layer is disintegrated, until it reaches a maximum value within few hours, then it slows down for the rest of hydration period [10]. This temperature rise results from the speed up of C_3S hydration associated with the precipitation of calcium hydroxide. Eventually, the availability of reactants becomes limited as the very fine cement particles are depleted, thus the rate of the hydration reactions decreases and the rate of heat evolution declines slowly with time (through a diffusion-controlled stage). After a sufficiently enough time, the hydration reaction of C_2S is promoted and then causes an additional thermal contribution that can create a shoulder in the differential heat evolution curve. A steady formation of hydration products continues at a slow and nearly constant rate reaction rate (diffusion-controlled) over a very long period of time period which governs the late-strength gain rate and the concrete porosity. Within the typical 28-day curing period, almost 65% of the hydration reactions are completed and 90% of the target compressive strength is achieved [10]. Decreasing w/c ratio increases the height of the major thermal peak [17]. Adding set-accelerating or retarding admixtures can cause a shift in the thermal peak of the differential heat evolution curve. Similarly, the thermal peak can be shifted and lowered by adding supplementary cementitious materials (SCM) due to their retarding effects and the reduction in cement content (which is replaced by an equivalent amount of SCM).

In structures involving mass concrete the temperature development can lead to more severe thermal cracking problems which are caused by developing thermal stress (that may exceed concrete strength) resulting from the temperature gradient [18]. This occurs since mass concrete involves a high temperature rise and temperature gradients within structure [19]. In mass concrete, a temperature rise of about 4.6 °C is caused by each 100 kg of cement addition [20]. The high temperature rise within the first three days, followed by a subsequent cooling stage causes shrinkage problems and cracking. Managing such a temperature rise in mass concrete is an essential durability requirement. Casting mass concrete is controlled by setting a maximum temperature (at 57 °C (135°F) [21]) for obtaining the required compressive strengths and setting a maximum temperature difference within the structure (at 19.4 °C) to prevent thermal cracking [19]. Engineering approaches for controlling the temperature include proper mix design, the use of low heat generating cementitious mixtures (e.g. proper selection of cement type, the use of SCM and the use of chemical admixtures). Fly ash, natural pozzolans, and ground slag have a lower heat of hydration than Portland cement. Substituting cement by SCM results in a dilution effect (reducing the concentration of the main cement compounds (i.e. C_3S) in the cementitious materials which causes the main hydration peak). The heat contribution of SCM at early age are much lower than those from cement; their contribution is within the range of 15–50% of that of an equivalent weight of cement. The additions of slag and fly ash to mixtures of mass concrete can achieve about 2 °C reduction in the temperature peak for each 10% replacement of cement by SCM [20]. A 10% addition of silica fume (as a replacement of cement) can achieve a 50% reduction in the 28-days thermal expansions [22]. However, the reactivity of fly ash increases significantly when the concrete temperature exceeds the above mentioned temperature limit [18]. For concrete with cementitious content higher than 250 kg/m^3, the temperature peak may exceed 60 °C and hence fly ash becomes ineffective in reducing the heat release in mass concrete. In general, the use of fly ash and ground granulated blast-furnace slag retard the setting of cement. Additionally, the rates of cement hydration and heat evolution in mass concrete can be reduced by the use of phase changing material such as barium oxide [23].

Concrete deuteriation resulting from thermal cycling effects in the presence of moisture is associated with internal stresses from the expansion of ice during the freezing cycle. This impact can be mitigated by minimizing free moisture content in concrete. Reducing water penetration in concrete can be achieved by external and internal waterproofing systems [24, 25]. Integral (or internal) waterproofing materials are added to concrete mix in order to reduce water penetration. These include hydrophilic pore blocking materials [26] and hydrophobic pore lining materials [27]. Recently, a new patented internal waterproofing Multi-Crystallization Enhancer (MCE) that combines hygroscopic, hydrophilic and hydrophobic materials has been used to reduce concrete porosity and enhance concrete durability [28, 29]. The theoretical analysis of MCE thermal performance is based on managing thermal effects and moisture content. The hypothesized mechanism of the MCE for controlling temperature, humidity and water phase change within concrete is based primarily on its dynamic crystallization mechanism. The setting mechanism of the MCE is based on the reactions of its active ingredients with cementitious constituents to form pore blocking crystals of hygroscopic and hydrophilic types [28]. These crystals result in major reductions in concrete porosity and water penetration as reported in a previous publication [29]. Furthermore, when exposed to moisture (in vapor or liquid phases), these crystals can expand and causes a further reduction in porosity [29]. The functioning mechanism of the MCE is based on (1) consuming available moisture through additional crystal growth and then releasing it back through its reversibility, (2) storing thermal energy in crystal growth by water adsorption and then releasing it back through its reversibility, (3) minimizing water penetration into the pores and (4) allowing concrete breathing through MCE performance of partial blocking mechanism [28]. As consequences of these capabilities of the MCE, water freezing within pores is significantly reduced or prevented by eliminating the availability of water and hindering the adhesion of ice on to the cementitious surface since icephobocity is corelated to hydrophobicity [30].

The role of traditional integral crystalline waterproofing materials (crystalline powder admixtures) in reducing concrete deterioration under cycles of freezing and thawing has been reported in previous papers [31, 32]. Additionally, the ability of topical treatment of concrete surface using dual-crystallization waterproofing engineered treatment (DCE) in reducing thermal impacts has been reported in other papers [33, 34]. No previous work has been published on the effect of the MCE aqueous solution on concrete resistance against cycles of freezing and thawing. It is also worth to mention that previous research and review articles investigating and surveying the durability of concrete did not report the effects of crystalline waterproofing materials on managing the thermal impacts of concrete curing process [35–39]. None of the recently published articles on crystalline powder admixtures has highlighted any role for these admixtures in managing thermal effects of cement hydration in normal or mass concrete [31, 40-43]. The functionality of the patented Multi-Crystallization Enhancer (MCE) as a waterproofing aqueous solution [28] has been demonstrated in a previous publication [29]. This paper aims at investigating the secondary role of MCE for managing and mitigating the thermal effects on concrete and follows a recommendation stated in the previous publication [29]. The experimental work involved investigating the effects of adding the MCE on the thermal behaviors of (a) cement hydration under normal standard curing condition, (b) curing of concrete under freezing conditions (c) curing of mass concrete (d) resistance of concrete against cycles of freezing and thawing, and (e) concrete conductivity (thermal and

electrical). The investigated experimental parameters included rate of heat release, temperature profiles, compressive and flexural strength, temperature-time factor (TTF), percentage mass change, percentage length change, percentage relative dynamic modulus, thermal conductivity and total charge passage.

2. Experimental work

Typical concrete materials were used in casting the required control specimens. Type I Portland cement conforming to ASTM C150 was used as the binder. Class C fly ash was used as a partial replacement of cement. The fly ash conformed to ASTM C618–12 and ASTM C989 with a specific gravity of about 2.6. In another test, slag was used as additional SCMs (together with fly ash) replacing another part of cement. The slag conformed to ASTM C-989 with a specific gravity of 2.8. Crushed limestone aggregates with an average Nominal Maximum Aggregate Size (NMAS) of 2.54 cm, obtained from the Martin Marietta Ames Mine, were used as coarse aggregates. Natural sand from the Hallett Materials North Des Moines pit were used as fine aggregates. The gradings of coarse and fine aggregates are listed in Table 1. The air entrainment and the water reducing agents were obtained from Euclid Admixture (Cleveland, Ohio, USA), GRT SA-50 and GRT 400-NC, respectively. In the enhanced concrete specimens, a patented aqueous solution of MCE manufactured by International Chem-Crete Corporation (Richardson, Texas, U.S.A.) was used. It consisted of three integrated active ingredients made of hygroscopic, hydrophilic and hydrophobic constituents as described in a recent patent [28]. The total solid content of MCE was about 15%, the specific gravity was 1.1, and the viscosity was 2.4 centipoise [28]. The MCE was added to the mixing water at a dosage of 2% of cementitious materials, as recommended by the material technical data sheet.

The concrete mix designs were identical to those used in a previous publication for studying the characteristics of MCE [29]. The main mix design was C4-WRC20 prescribed by the Iowa Department of Transportation as listed in Table 2 [44]. The values of water to cement (w/c) were within a range of 0.37–0.45. For one field experiment, a ready-mix of high-performance concrete of grade D (HPCD) with a w/c of 0.42 and a slump of about 7.6 cm was obtained from Standard Ready-Mix Concrete Co (Sioux City, IA, USA). In cement hydration experiments, three types of pastes were tested. These include (1) 100% Portland Cement, (2) a cementitious mixture composed of 80% Portland Cement and 20% Fly ash and (3) a cementitious mixture of 50% Portland Cement, 20% Fly ash and 30% slag.

The types of experiments, the experimental parameters, the applicable ASTM procedures and the mix design information are listed in Table 3. Experiments of hydration kinetics were made at the National Concrete Pavement Technology Center at Iowa State University, Ames, Iowa, USA. The rest of the experiments were made in the Construction Material Testing (CMT, Des Moines, Iowa, USA), with data testing certificates.

The rates of cement hydration and heat evolution were measured for control and MCE-dosed cement paste with a w/c ratio of 0.40 using three types of cementitious mixes including 100% Portland Cement, 80% Portland Cement modified with 20% Fly ash and 50% Portland Cement modified with 20% Fly ash and 30% slag (see Table 3). The experiments were done using calorimetry testing according to the procedures of ASTM C1702–17. Then, the curves of differential heat evolution as functions of curing time were plotted for the three mixes.

The effect of the MCE on controlling the temperature rise and the internal temperature difference in mass concrete was tested using control and MCE-dosed concrete mixtures of C4-WRC20 mix and a w/c ratio of 0.37 (see Table 2 for concrete mix design). The specimens were rectangular shape 1.52 × 1.52 × 1.22 m. Thermal probes were placed into each specimen at various specified locations. The specimens were left in the ambient conditions to cure in the surrounding weather conditions. Curing was conducted outdoors (exterior) with no special precautions (such as a curing compound, burlap, etc.). The temperatures were recorded automatically during the initial curing period and then temperature curves were prepared for each specimen. Additionally, cores (two replicates) after 35 days of curing were created from each

Table 1
Gradings of coarse and fine aggregates (% retained).

Sieve opening (standard No.)	Coarse aggregates	Fine aggregates
−12.5 mm (1/2 inch)	54%	0
9.5 mm - 4.75 mm (No. 4)	36%	5%
4.75 mm (No. 4) 2.36 mm (No. 8)	2.5%	8%
2.36 mm (No. 8) 1.18 mm (No. 16)	0.9%	14%
1.18 mm (No. 16) 600 μm (No. 30)	0.7%	32%
600 μm (No. 30) 300 μm (No. 50)	0.6%	31.1%
300 μm (No. 50) 150 μm (No. 100)	0.3%	9.9%

Table 2
concrete mix design (C4-WRC20) as prescribed by Iowa Department of Transportation [44].

Component	Amount (SI units)
Cement	222.9 kg
Fly ash	55.8 kg
Coarse aggregates	691 kg
Fine aggregates	684 kg
Air entrainment	6%
Water reducer per cubic yard	118 ml
w/c	0.37–0.45

Table 3
investigated experimental parameters and conditions in each experiment.

Study	Experimental Parameter	Procedure	Cementitious Mixes	w/c
Cement Hydration under normal curing condition	rate and cumulative heat release	ASTM C1702–17	- Portland Cement 100% - Portland Cement modified with 20% Fly ash - Portland Cement modified with 20% Fly ash and 30% slag	0.40
Curing of Mass Concrete	- temperature profiles - temperature-time factor (TTF) - compressive strength - splitting tensile strength	ASTM C39 ASTM C496 C1064	C4-WRC20	0.37
Curing under freezing conditions	- temperature profiles - compressive and flexural strengths - relative dynamic modulus	Modified ASTM C666 ASTM C1074 ASTM C39	C4-WRC20	0.40
Cycles of Freezing and Thawing	- temperature profiles - percentage mass change - percentage length change - percentage relative dynamic modulus	ASTM C666	C4-WRC20	0.40
Thermal Conduction	- thermal Conductivity and resistivity	ASTM C168	C4-WRC20	0.45
Electrical Conduction	- total electrical charge passage	ASTM C1202	C4-WRC20	0.4

specimen (control and MCE-dosed concrete) and then tested for compressive strength according to ASTM C39 and splitting tensile strength according to ASTM C496.

The concrete curing under freezing conditions was investigated using control and MCE-dosed concrete mixtures of C4-WRC20 mfixes at w/c ratio of 0.40 (see Table 2 for concrete mix design). The specimens were cast and cured for 24 h in a moist (SSD) condition at a temperature range of −18°. Specimens were cast into 7.62 × 7.62 × 40.6 cm beams to fit the freezing chamber. Then, the specimens were subjected to freezing conditions at a constant temperature of −45 °C (Modified conditions of ASTM C666) for 90 days. In specimens utilized for temperature measurements, thermal probes were placed into each specimen at two depths of 1.27 and 3.81 cm below the surface of concrete. Then, curves of temperature profile were plotted showing the standard errors on the curves as error bars. A similar experiment was performed by placing the specimens in the freezing chamber immediately after the initial casting step. However, the specimens froze within 90 min showing visible frozen crystals of water on the surface of the specimen. In addition, concrete strength gain was monitored by measuring the temperature-time factor (TTF) and the compressive strength development using the maturity method according to ASTM C1074. TTF factors were established by allowing specimens to cure in ambient conditions prior to compressive strength testing, per the ASTM test method. TTF was determined by allowing the specimen to achieve a certain internal temperature at a certain age (usually in hours), then testing the specimen for strength gain and correlating the temperature to the specimen strength and age in hours.

Additionally, concrete specimens of control and MCE enhanced concrete (two replicates for each) were aged to 90 days in the freezing chamber. The concrete mix design was similar to an IDOT C4 mix design (the mix contained 269 kg of Type I/II cement with no-fly ash, and a 50/50 blend of fine to coarse aggregates). The mix was created at a w/c ratio of 0.42. The specimens were aged to 90 days in the freezer chamber and then, coupons were cut from the specimens and tested for compressive strength and flexural strength (center point loading). At the end of the 90 days period, the relative dynamic modulus for each specimen (control and MCE-dosed specimen) were determined as averages of two replicates.

Rapid freezing and thawing was made on control and MCE-dosed C4-WRC20 concrete with a w/c ratio of 0.40 (see Table 2 for concrete mix design). Specimens were cast into 7.62 × 7.62 × 40.6 cm beams to fit the freezing and thawing chamber. The freezing and thawing experiments were performed according to ASTM C666 [45]. The procedures of the ASTM C666 testing conditions were modified to utilize more extreme temperatures: by cycling between −53 to 22 °C (instead of the range of −29 to 4.4 °C, specified by the ASTM C666). After initial standard curing period for 24 h in laboratory conditions at a constant temperature range of 18 °C to 24 °C, the specimens were placed in the freezing and thawing chamber. The specimens were cycled through 300 cycles of freezing and thawing, averaging 8 h per cycle. At the selected numbers of cycles (using intervals of 30 cycles), measurements were taken for mass, length and dynamic modulus for control and MCE-dosed specimens (three replicates of each). Then, curves of average percentage changes in these durability parameters were plotted, with standard errors represented on the curves as error bars.

Additionally, for similar types of specimens (C4-WRC20 concrete with a w/c ratio of 0.40, see Table 2 for concrete mix design) and conditions of freezing and thawing cycles, the temperatures of control and MCE-dosed specimens were measured at two depths, using three replicates for each. This was done by placing thermal probes into the concrete specimens at two depths of 1.27 and 3.81 cm from the surface. Then, curves of average temperatures at the two depths versus time were plotted versus times for each of the two cases. The standard errors in these measurements were shown as error bars on these curves. These experiments for internal temperature measurements were repeated on two groups of specimens, using three replicates for each specimen.

The thermal and electrical resistivities were measured for control and MCE-dosed C4-WRC20 concrete with w/c ratio of 0.45 (see Table 2 for concrete mix design). The thermal conductivity was measured according to the definitions in ASTM C168 “Standard Terminology Relating to Thermal Insulation” [46]. The thermal conductivity was determined after establishing a steady-state heat conduction through a unit area of the concrete specimen, induced by a constant temperature gradient in a direction perpendicular to the area within a 2.54 cm thick panels. Specimens were 7 day of age cylinders (10.2 × 20.3 cm) cut to a disk size of 5.1 cm.

Experiments for studying the effect of the MCE on electrical resistance of concrete (or resistance against chloride ion penetration) were made according to ASTM C1202 using C4-WRC20 concrete at a w/c of 0.40 (see Table 2 for concrete mix design) after 7 days of curing. One side of the concrete specimen was subjected to a standard solution of NaOH (with 0.3 normality), while the other side was subjected to a standard solution of NaCl (3.0% by mass). The solutions were prepared in distilled water and applied at ambient temperature. The electrical currents passing through control and MCE-dosed concrete specimens were measured as functions of time, then the total charge passage was estimated from the area under the current-time curve for six hours (as specified by ASTM C1202).

3. Results and discussion

3.1. Cement hydration

Fig. 1 shows curves of rate heat release and cumulative heat release during the first 48 h for three cementitious mixtures including Portland cement, Portland cement modified with 20% fly ash and Portland cement modified with 20% fly ash and 30% slag. Fig. 1 shows that all types of mixtures lead to a nearly similar characteristic shape of hydration curves that is comparable to those reported in literature for various cementitious mixtures [11–15]. Such a characteristic curve shape reflects the physicochemical mechanisms of cement hydration kinetics, which is controlled by the mixture temperature [16]. These mechanisms include particle dispersion in the mixture and ion dissolution (upon mixing with water) as well as diffusion, particle coagulation, water phase changes and hydration chemical reactions during the subsequent stages [9]. The exothermic actions [11–15] include (1) a fast heat evolution from the heat of solution that occur within the first few minutes from the moment of mixing cement with water [13], (2) heat evolution from the formation of ettringite through a highly exothermic reaction which occurs within the first few hours coupled with a minor exothermic actions from the dissolution of C_3S and the early formation of C-S-H and (3) the heat of reactions of the cement constituents. Fig. 1 shows that for all types of the investigated mixtures: upon mixing the cementitious mixture with water, a large sudden thermal peak is obtained, which is attributed to the release of heat of solutions of rapid soluble materials such as aluminates and sulfates [13] and the heat of formation of ettringite. This is then followed by an induction period of slow reactions leading to the formation of a layer of hydration products around the powders of the cementitious mixtures as reported in previous literature [10]. Subsequently, the heat release is accelerated gradually after the induction period as the formed protective layer around the cement particles is disintegrated and then it reaches a maximum value within few hours. Such an increase is attributed to the acceleration of the hydration of C_3S, which is associated with the precipitation of crystals of calcium hydroxide. It is known that the heat liberation coming from the hydration of C_3S composes about 50% of the full heat release of the cement hydration, and it reacts at a much faster rate than C_2S (more than five times faster) [10]. The subsequent hydration reaction of C_2S, that is promoted after a sufficient time, generates an additional thermal contribution and creates a shoulder after the main peak. The hydration of C_2S releases nearly half of the heat released from the hydration C_3S. Then, the rate of heat release decreases, during the post-acceleration

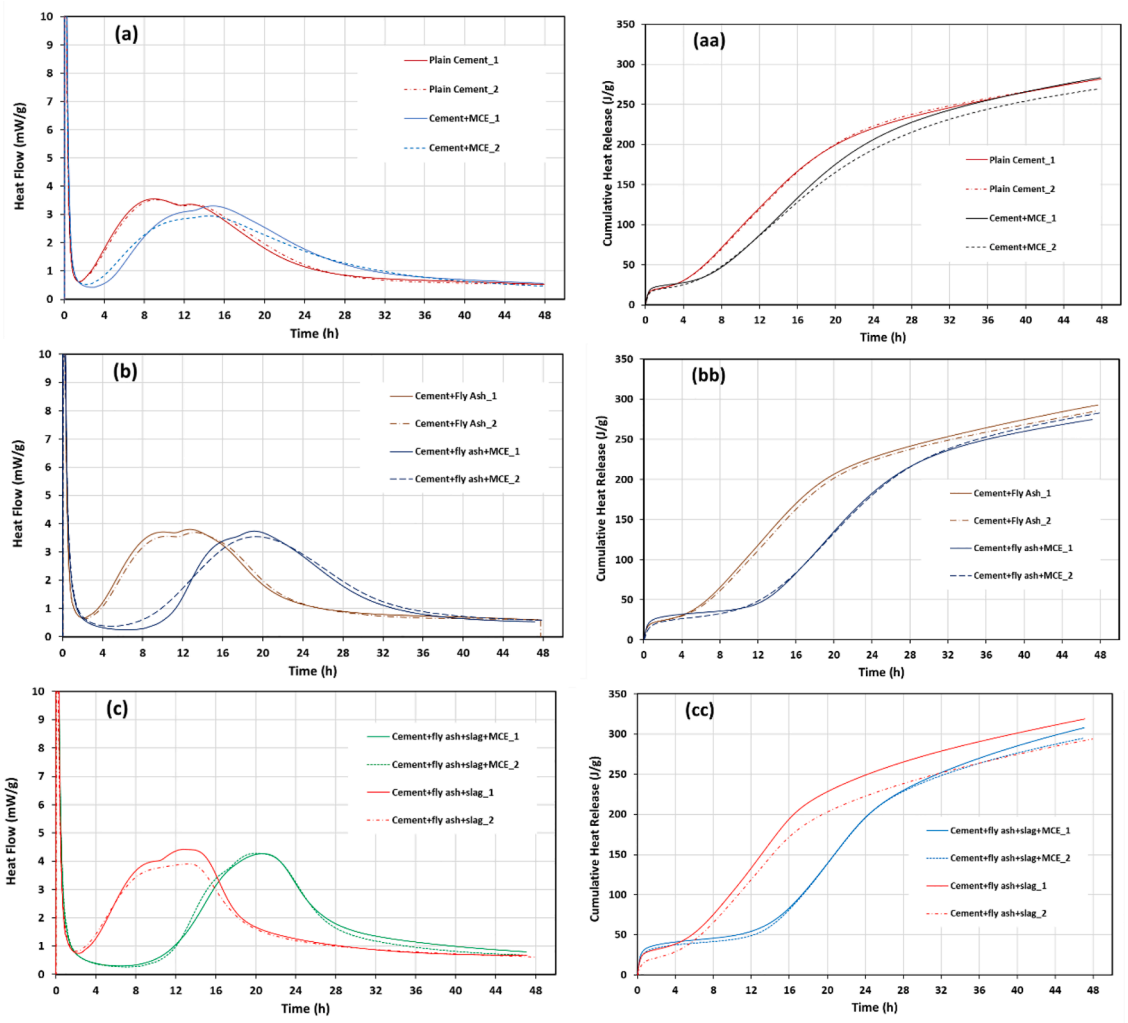

Fig. 1. Reate of heat release (mW/g) and cumulative heat release (J/g) during the first 48 h for three cmenetitios mixes including 100% Portalnd cement (a and aa), (b) Portland Cement modified with 20% Fly ash (b and bb) and (c) Portland Cement modified with 20% Fly ash and 30% slag (c and cc).

stag, leading to a steady formation of hydration products which is attributed to the diffusion-controlled stage and to the depletion of the hydration reactants and the very fine cement particles. This stage continues at a slow and nearly constant rate reaction rate over a very long period of time and it governs the late-strength gain rate and the concrete porosity. These experiments were performed with a w/c ratio of 0.40: it is reported in literature that decreasing w/c ratio increases the height of the major thermal peak [17]. Adding set-accelerating or retarding admixtures can cause a shift in the thermal peak of the differential heat evolution curve. Fig. 1 also shows that the thermal peak is shifted by adding supplementary cementitious materials (SCM) as reported in literature. This is due to the retarding effects associated with the reduction in cement content within the mixture (i.e. reduction of the availability of C_3S) since part of the cement is replaced by an equivalent amount of SCM.

Table 4 lists the net average values of cumulative heat release during the 47 h and the equivalent times of the heat evolution peaks for the investigated three mixtures. The cumulative heat release depends on the chemical composition of mixture. The addition of the MCE to cement causes a rightward shift in the cumulative heat release curve which reflects the ability of MCE to store the released heat for a longer period of time in the first two days. This enhances the process of casting and curing concrete under sever cold conditions as shown in the experimental results in Section 3.3. On the other hand, the values of the net cumulative heat release at 47 h are within −1.27 to −3.45% for MCE dosed concrete. This indicates that the MCE does not interpose the cement hydration process as the heat evolution from the exothermic reactions are very close for cases with and without the MCE. The

Table 4
Results of Calorimetry experiments on the kinetics of hydration of three types of cementitious mixes at a w/c ratio of 0.40.

Cementitious Mix	Parameter	Unit	Control sample	MCE-dosed sample	% Difference between MCE and control specimens
Portland cement	Total Heat Release within 47 h	J/g	279.9	274.9	−1.79%
	Time of the peak	hr	9.31	14.68	57.7%
Portland cement modified with 20% fly ash	Total Heat Release within 47 h	J/g	287.6	277.7	−3.46%
	Time of the peak	hr	10.25	19.2	87.3%
Portland cement modified with 20% fly ash and 30% slag	Total Heat Release within 47 h	J/g	305.1	301.2	−1.27%
	Time of the peak	hr	13.1	20.3	55%

pozzolanic effect (reactions of fly ash or slag with lime from the hydration of cement) adds to the heat output as observed in Table 4 when comparing the cumulative heat release from Portland cement with those containing SCM. This is attributed to the heat of reaction of pozzolans with calcium hydroxide.

Similar to the addition of SCM, adding MCE to any of the cementitious mixture causes a similar rightward shift in the time of the heat rate peak. The percentage shift in the peak ranges between 55% to 87% depending on the types and the percentage of the SCM in the mixture. Similar heat evolution curves, with similar time shifts were reported in previous literature when a waterproofing powder admixture was used [47]. It has been reported that waterproofing admixtures causes a shift in the rate of heat release peak and extends the release of heat over a longer period of time, which assists in creating better conditions for cement hydration [47]. The additions of the MCE, SCM or powder admixtures cause a retarding effect on the cement hydration as indicated by shifting the curves of these cases rightward; since the active ingredients participate in the physicochemical interactions with cement particles [41]. This normally leads to structural changes in the phases of the hydrates and causes process modifications in the hydration reactions (e.g. variations in the rate of nucleation and growth kinetics of the hydrates) [41]. This retarding effect is reflected in the temperature development curves of cement hydration kinetics. Furthermore, a mild deceleration of the hardening of concrete during the first 28 days had been reported for powder crystalline admixtures [48]. Additionally, the use of waterproofing powder admixtures of fluorosilicate types was reported to lead to a significant set retarding [49]. The addition of minor amounts of fluorosilicate admixtures (0.5% dosage) lead to delay in the setting time for about 2.5 h [50]. This was attributed to precipitations from the reactions of active ingredients that hindered the cement hydration [50]. Similar retarding effects were also reported for other non-silicate based waterproofing powder admixtures [41]. It has been reported that "hindering the hydration inhibits the rapid increase of the cement hydration heat before hardening due to the thermodynamic heat-absorbing effect" [50]. Thus, the retarding effect of waterproofing admixtures can lead to lower chance of cracking and reduces the premature moisture loss [47]. The level of retarding is dependent on the types and amounts of the additives in the mixtures and on the w/c ratio. It has been reported that the effective thermal management during the initial cement hydration induced by adding crystalline waterproofing materials to concrete mixes reduces the premature losses of moisture and create a more durable structure with reduced shrinkage [47].

3.2. Curing mass concrete

Fig. 2-a shows the measured temperatures within the time scale of 72 h comparing those for control and MCE-dosed concrete, at various locations in mass concrete specimens (locations of temperature sensors are shown in Fig. 2-b). Figs. 3 shows two temperature curves (at two locations with maximum and minimum peaks) in MCE dosed mass concrete specimens for nearly full curing period (about 27 days). Fig. 2 shows that adding MCE causes a drop in the maximum temperature equivalent to about 6.7 °C. These obtained temperature peaks for both the MCE-dosed and control mass concrete are below the acceptable maximum temperature limit of 57 °C (stated as 135°F in [21]). This is essential since high temperature rises within the first three days and the subsequent cooling creates thermal stress and causes shrinkage problems [18]. This is attributed to the fact that the used control mix design (C4WR-C20) is suitable for mass concrete as it is made with 20% replacement of cement with fly ash. However, MCE resulted in much lower value of the maximum temperature. Adding MCE to the mixture of mass concrete results in lowering the temperature peak by about 6.7 °C. Fig. 4 shows temperatures at 10 cm depth (from the top surface) as function of time obtained from a field test for control and MCE-dosed mass concrete. These results confirm that MCE addition to mass concrete lowers the maximum temperature by a similar drop of 6.7 °C at the indicated location. Such a reduction in the maximum temperature requires the addition of about 35% fly ash as indicated by recent study [20]: since the pozzolans-to-binder ratio lead to a reduction in the temperature by about 2 °C/10% of pozzolans (slag and fly ash) in mass concrete since the early-stage heat contributions of SCM are within the range of 15–50% of that of an equivalent weight of cement [20]. This decrease of maximum temperature by the addition of MCE can permit increasing the cement content in mass concrete while maintaining low maximum temperatures, as it has been reported that a temperature rise of about 4.6 °C is caused by each 100 kg of cement addition [20]. More importantly is that the maximum allowable temperature difference between the center and surface of the mass concrete section must not exceed 19.4 °C (35°F). When the difference between the temperature at the hottest portion point and that at the surface is high; thermal cracking occurs when the thermal stress resulting from the temperature gradient exceeds the concrete strength [18]. Figs. 4 shows that the maximum temperature difference in MCE-dosed concrete (between locations 1 and 5) is equivalent to about 10 °C which is nearly half of the set maximum temperature difference. For the control mass concrete, the maximum temperature gradient is equivalent to about 13 °C. This indicates that MCE achieves larger reduction in the temperature gradients in mass concrete than the control specimen. This also indicates that the effective thermal management of MCE is not limited to lowering the maximum temperature (peak) but it also decreases the internal temperature difference, which is an important thermal parameter in controlling mass concrete durability through minimizing thermal shrinkage and cracking. Overall, the use of MCE maintains the temperature in mass concrete below the allowable temperature limits of temperature peak and internal difference and controls the temperature rise and the temperature gradient between various locations with the mass concrete. In addition to these reductions, Fig. 2 shows that the addition of MCE to mixtures of mass concrete shifts the time at which these temperature peaks occur by

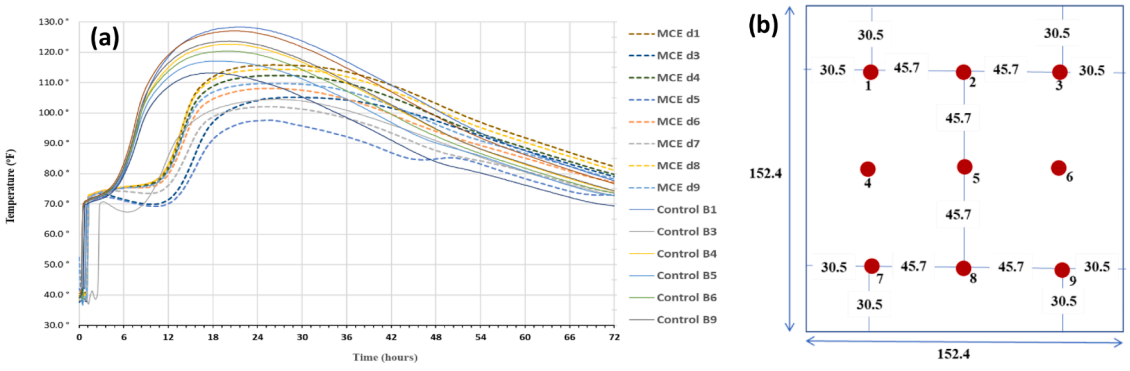

Fig. 2. Temperature at various locations in mass concrete specimens, comparing those for control and MCE-dosed concrete, using C4-WRC20 at w/c ratio of 0.37 (a), and the locations of the temperature sensors within the specimen (b).

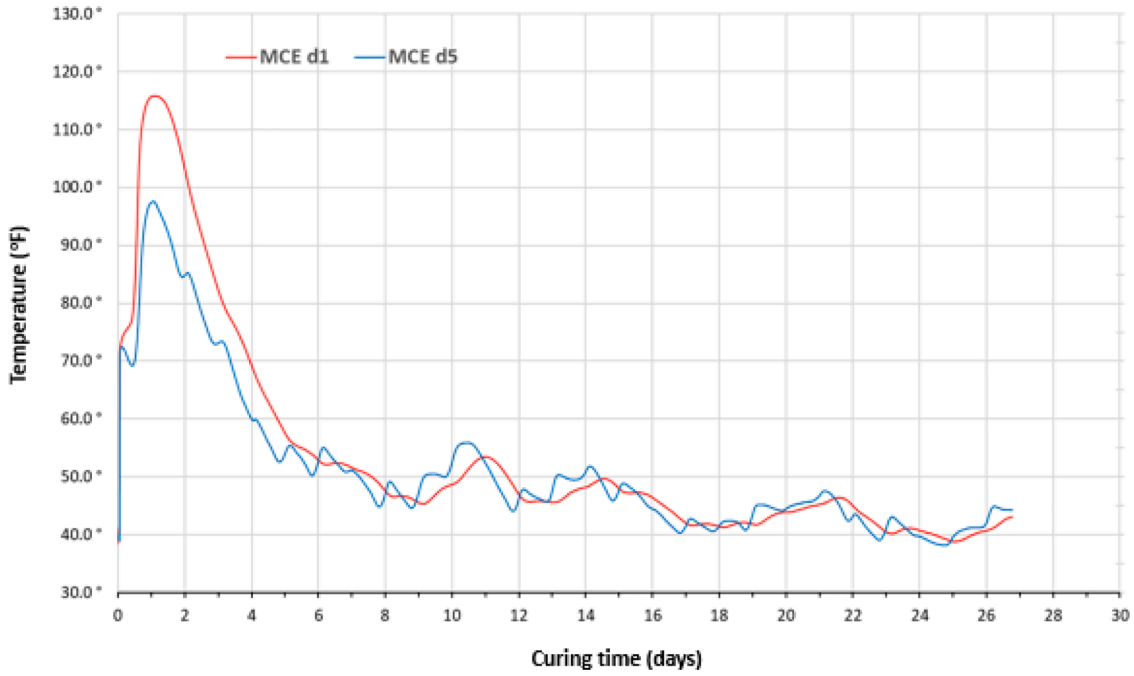

Fig. 3. maximum and minimum temperatres (at locations of 1 and 5 as shown in Fig. 2) within MCE-dosed mass concrete specimens using C4-WRC20 at w/c ratio of 0.37 for nearly full curing time.

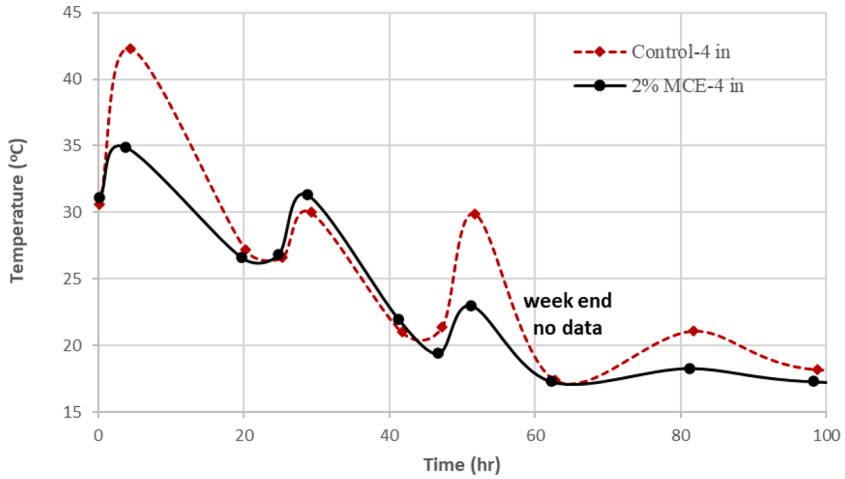

Fig. 4. Temperature versus time at 10 cm depth in mass concrete using Ready Mix HPCD mix design, comparing MCE enhanced and control specimen.

about 7 h. This is an essential positive behavior for mass concrete since it assists in controlling the rate of heat evolution at early stages. The MCE mechanism can be explained by the following roles (1) the moisture management and control of water loss at early stages resulting from the large heat release from the exothermic cement hydration reactions. (2) MCE is believed to lower the rate of heat generation for concrete and (2) MCE has an initial retarding effect from one of its ingredients, which contributes positively in controlling the rate of heat generation from cement hydration. In addition, MCE is believed to increase the heat capacity of MCE treated concrete, a characteristic that is going to be investigated in future testing.

MCE performance in managing thermal effects in mass concrete enhances the compressive strength by 10% as listed in table 5. This is attributed to the role of MCE in maintaining the maximum temperature below the set maximum (57 °C) which is reported to be crucial for obtaining the required compressive strengths [19]. It is also attributed to the role of MCE in maintaining the maximum temperature difference within the structure below the set limit of 19.4 °C to prevent thermal cracking.

Table 5
compressive strength and splitting tensile strength for control and MCE-dosed mass concrete (C4-WRC20 mix and w/c ratio of 0.37) at the age of 35 days.

Parameter	Control mass concrete	MCE-dosed mass concrete
Compressive strength	27.6 MPa	30.4 MPa
Splitting tensile strength	1.6 MPa	1.2 MPa

The effects of MCE on the strength and maturity of mass concrete are shown in Fig. 5 comparing two baseline mortar mixes with two mortar mixes dosed with MCE at a dosage of 2%. Maturity curves were created using mortar mixes. The two sets of mixes varied by their aggregate ratios of coarse aggregate to fine aggregate (CA/FA). One mix was a 55/45 blend of CA/FA, while the second mix was a 60/40 blend of CA/FA. The results shown in Fig. 5 confirm that a slower strength gain in early

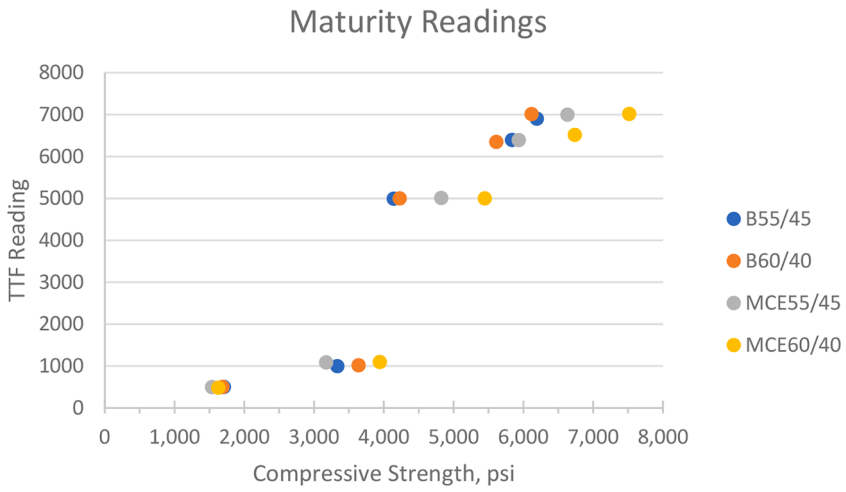

Fig. 5. Maturity results of mass concrete comparing two baseline mortar mixes with two mortar mixes dosed with MCE at a dosage of 2%. One mix was a 55/45 blend of CA/FA, while the second mix was a 60/40 blend of CA/FA.

hydration and a higher compressive strength at 28 days for mixes with the MCE than those for control mixes.

3.3. Hydration under freezing conditions

Fig. 6 shows concrete temperatures at two locations (top at 1.27 cm below surface and middle at 3.81 cm below concrete surface) during curing under continuous freezing surroundings at −45 °C for 90 days, after allowing the concrete specimen to cure at normal conditions for an initial 24-hours curing period. The shown error bars confirm the repeatability of these results. Fig. 6 shows that the temperature of control specimen drops below the freezing temperature after the second day for the top location and after the third day for the middle location. On the other hand, the temperature of MCE-dosed specimen remains above the freezing temperature during the first month for the top location and during the second month for the middle location. Then, the temperatures of MCE-dosed specimen at the two locations remain just at, or very close to, the freezing temperature for the subsequent periods (till 90 days). It is clear that the temperatures of MCE-dosed specimen at the two locations remain higher than the temperatures of control specimen at the two locations by about 5.5 °C. This behavior is associated with the ability of MCE to store the released heat from the initial cement hydration as explained in Section 3.1. This unique thermal role of MCE in preventing water freezing in fresh concrete for sufficiently long time enables it to play a major role in promoting cement hydration under severe cold condition. When water remains in liquid phase for about two months, the cement hydration reactions proceed to a nearly full curing and the process of strength development continues to achieve the required compressive strength. On the other hand, when the fresh concrete without MCE is subjected to severe cold conditions, the process of cement hydration is hindered by freezing water within 2–3 days. Preventing water freezing requires sufficient internal energy within the concrete specimen. Since under continuous cooling the specimens loose heat to the surrounding continuously at a rate that is governed by the high temperature difference between the surrounding and the specimen, then maintaining a reasonably high temperature in the specimens cannot be secured without having an internal source of energy within the specimen. In principle, the exothermic cement hydration reactions provide the main source of heat generation. However, the difference in thermal performance (under freezing conditions) between control and MCE-dosed specimens can be explained by having higher sources of heat generation within the MCE-dosed concrete that reduce the temperature drop significantly. These heat sources remain available to substitute the energy loss to the surrounding and hence manages the temperature of concrete during its curing stage. These heat sources include (1) heat release from the continuous slow hydration promoted through maintaining the availability of non-freezing water by MCE role, (2) heat release from the enthalpy change of the MCE crystallization reactions (i.e. from the MCE precipitation and hydration mechanisms), and (3) heat release from vapor condensation upon adsorbing moisture in the growth

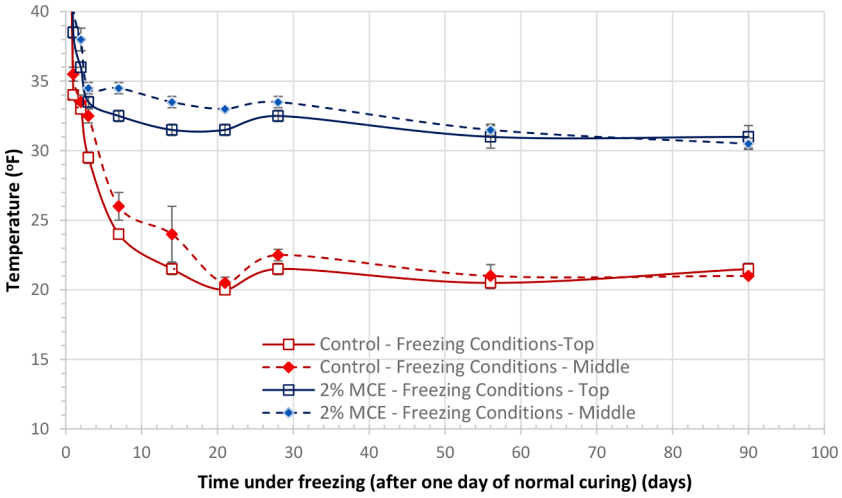

Fig. 6. Temperatures (top at 1.27 cm below surface and middle at 3.81 cm below concrete surface) of control and MCE-dosed C4WRC20 concrete specimen at w/c = 0.40 cured under continuous freezing surroundings at −45 °C, after allowing the concrete specimen to cure at normal conditions for an initial 24-hours curing period. The standard errors of two replicates are shown as error bars. (For interpretation of the references to colour in this figure legend, the reader is referred to the web version of this article.)

of hygroscopic crystals (from surrounding humid air). In addition to these heat generation terms, MCE reduces the thermal conductivity of concrete (see results in Section 4.5) and hence maintain a large fraction of heat generation available for promoting cement hydration.

These sources are secured when the fresh concrete mixture has been given a sufficient period to pass the setting period (and to jump over the heat evolution peak, see Fig. 1). Hence, when similar two specimens were placed in the freezing chamber under similar experimental conditions immediately after casting, the experiment failed and the curing process was not accomplished: the concrete did not have time to promote hydration reactions as the specimens froze within 90 min showing visible frozen crystals of water on the surface of the specimen and low internal temperatures were observed in both control and MCE-dosed specimens. This is attributed to the shortness of the available time for initial cement hydration and for insufficient initial heat evolution that can drive the remaining curing period. This is an indication that promoting hydration at the initial period (e.g. 24 h) by protecting the fresh concrete from extremely cold conditions through its setting period is essential to benefit from the MCE thermal role in preventing water freezing and promoting a continuous process of cement hydration.

3.3.1. Mechanical properties

As described above, the thermal role of MCE in maintaining water in liquid phase for about two months promotes continuing cement hydration and the development of concrete mechanical characteristics in terms of compressive strength, flexural strength and dynamic modulus: Table 6 compares the compressive strength and flexural strength for control and MCE-dosed C4WRC20 concrete specimens at w/c ratio of 0.42, cured under severe cold conditions of −45.6 °C for 90 days. The addition of MCE achieved a 20% increase in the compressive strength and a 30% increase in the flexural strength. These increases are attributed to the role of MCE in promoting cement hydration under severe cold conditions. Fig. 7 shows the projections of the compressive strength of control and MCE enhanced concrete samples, cured at severe cold conditions (at −45.6 °C) for 90 days, on a curve of compressive strength for control concrete cured at normal conditions (for C4WRC20 mix at w/$c = 0.42$), for data obtained from a previous publication [29]. It is clear that the thermal capability of MCE for preventing freezing of water within the pores of fresh concrete (see Fig. 6), gives it the ability to promote the hydration of cement under these freezing surrounding conditions but the level of curing is lower than that obtained under normal curing conditions. It is shown in Fig. 7 that the strength of the control specimen after 90 days curing under freezing conditions is nearly equivalent to that for similar concrete cured under normal condition, only for 7 days or less. This indicates that most of the strength development under freezing conditions for control sample is gained within the first 3 days before freezing (see Fig. 6). On the other hand, the 90-days compressive strength for the MCE-dosed concrete under freezing conditions is equivalent to that for similar concrete cured under normal condition, for nearly 20 days. These differences are explained by the ability of MCE to promote cement hydration reactions even if it is subjected to extremely cold conditions. In fact, Fig. 7 shows that the obtained compressive strength with MCE under severe conditions for 90 days, reaches about 90% of the compressive strength of non-treated concrete cured at normal conditions for 56 days. This is due to the aforementioned continuous sources of heat. Such heat sources counter the heat loss to the surrounding at −45 °C. However, it was shown that the temperature of the control sample dropped to a value below freezing within three days and remained at freezing conditions for the rest of the periods, a condition, which is well reported in the literature that it hinders cement hydration. This means that MCE can permit concrete casting under severe cold conditions if it passes the first 24 h. Similarly, after 90 days of subjecting the specimen to continuous freezing conditions (for the case with initial 24 h of normal curing), the relative dynamic modulus of control and MCE-dosed specimens were 34.06 and 39, respectively. Based on historical data with a similar mix design (C4WRC20), the MCE-dosed specimen achieved 99th percentile while the control specimen achieved 94th percentile of a passing result. A traditional ASTM C-666 test (cycles of freezing and thawing) fails when the resilient modulus drops below the 60th percentile. The difference in the observed resilient modulus readings represents a 15% increase in performance in the MCE-dosed specimen over the control specimen.

Table 6
compressive strength and flexural strength (average of two replicates) for concrete samples using C4WRC20 mix at w/c ratio of 0.42, cured under severe cold conditions −45.6 °C for 90 days.

Parameter	Testing Condition	Control Specimen	MCE Enhanced Concrete	Percentage Difference
Compressive Strength (MPa)	2 × 2 inch cube	32.5	38.9	20%
flexural strength (MPa)	Center point loading	4.34	5.55	28%

3.4. Resistance to cycles of freezing and thawing

The aforementioned thermal behavior of MCE for resisting freezing during curing under severe cold conditions is further supported by measuring the effect of MCE on three parameters of dimensional stability under repeated cycles of freezing and thawing tested according to ASTM C666 with cycling done between more severe conditions than those specified in ASTM C666. Figs. 8-a and b show curves of percentage mass change and percentage length change as functions of number of freezing and thawing cycles, respectively, for control and MCE dosed concrete with 2% MCE, (C4WRC20 at w/c of 0.40). The shown error bars confirm the repeatability of these results. Adding MCE to concrete decreases percentage mass change and percentage length change. Fig. 8-a shows that the percentage mass change is reduced significantly at all numbers of freezing and thawing cycles. The reductions in percentage length change as functions of number of freezing and thawing cycles shown in Fig. 8-b are lower than those obtained with the similar crystalline waterproofing material when applied as a topical surface treatment DCE [33]. Additionally, Fig. 9 shows curves of percentage relative dynamic modulus as a function of number of freezing and thawing cycles from the same tests. The percentage relative dynamic modulus for MCE-dosed concrete is higher than that for control concrete indicating higher dimensional stability with MCE. Table 7 lists the percentages reductions in percentage mass change and percentage length change after 300 cycles: MCE resulted in about 92% reduction in the mass loss, and 15% reduction in the percentage length change in addition to about 17% increase in the relative dynamic modulus. These results show that MCE has the potential to increase concrete resistance against damages from cycles of freezing and thawing by enhancing concrete dimensional stability.

These increases in thermal durability parameters of MCE-dosed concrete are attributed to the ability to prevent water freezing under cycles of freezing, based to the aforementioned mechanisms. This hypothesis was confirmed by measuring the internal temperatures of the control and MCE-dosed concrete specimens at two locations. Fig. 10 shows the internal temperature of concrete specimens (at 1.27 cm depth below the surface) for control and MCE-dosed during freezing and thawing cycles, obtained from two repeated experiments. It is clear that the internal temperature of control specimen during the freezing cycle always drops below freezing (equivalent to about −11 °C in group one and about −7.8 °C in group two). On the other hand, the internal temperature of the MCE-dosed specimen never drops below freezing temperature (nearly always > 40°F). Similar charts were obtained for the temperatures at a depth of 3.81 cm, with minor temperature variations from those for the 1.27 cm depth. Additionally, the hydrophobicity of MCE system minimizes ice adhesion and hence assists in minimizing

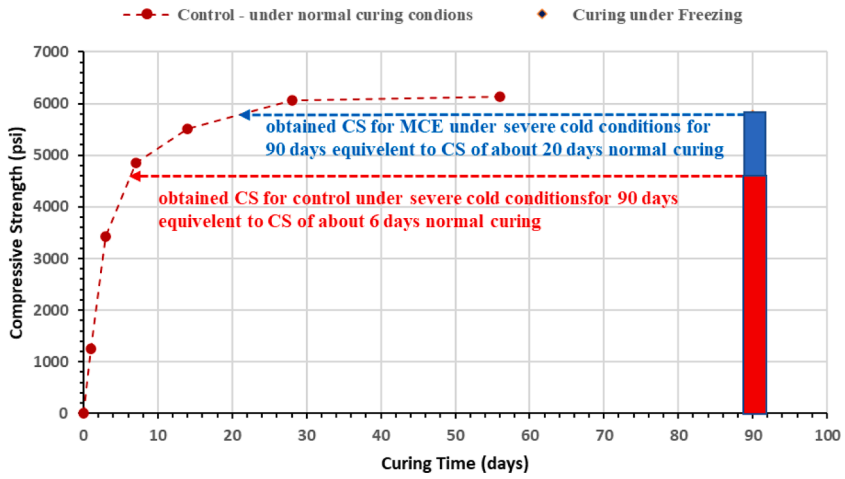

Fig. 7. compressive strength of control and MCE enhanced concrete samples (cured at T below −45.6 °C for 90 days) projected on a curve of compressive strength for control concrete cured at normal conditions all data are for C4WRC20 mix at w/c = 0.42.

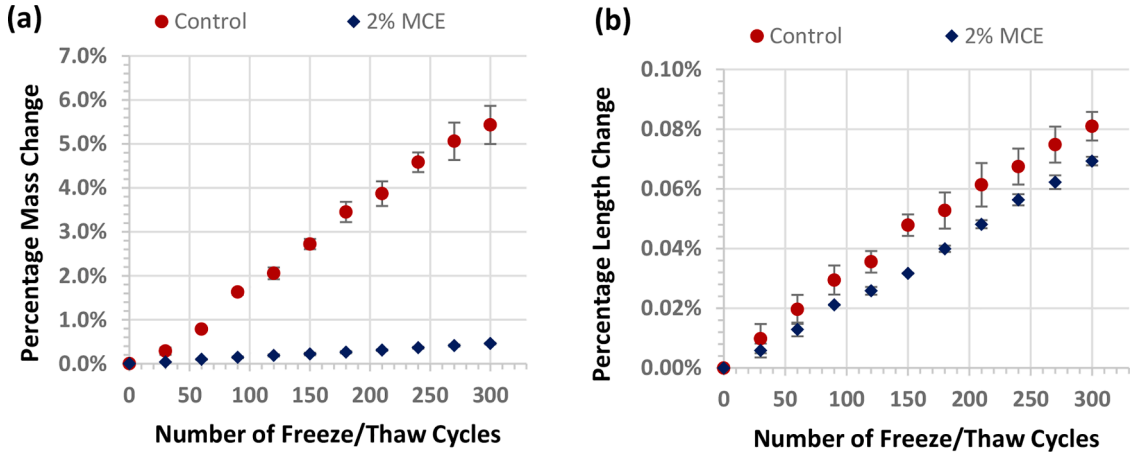

Fig. 8. curves of percentage mass change (a) and percentage length change (b) versus number of freezing and thawing cycles using modified ASTM C666 (i.e. cycling under more extreme temperatures of −53 to 22 °C), comparing control sample with concrete mixed with 2% MCE, (C4WRC20 at w/c of 0.40). The standard errors of three replicates are shown as error bars.

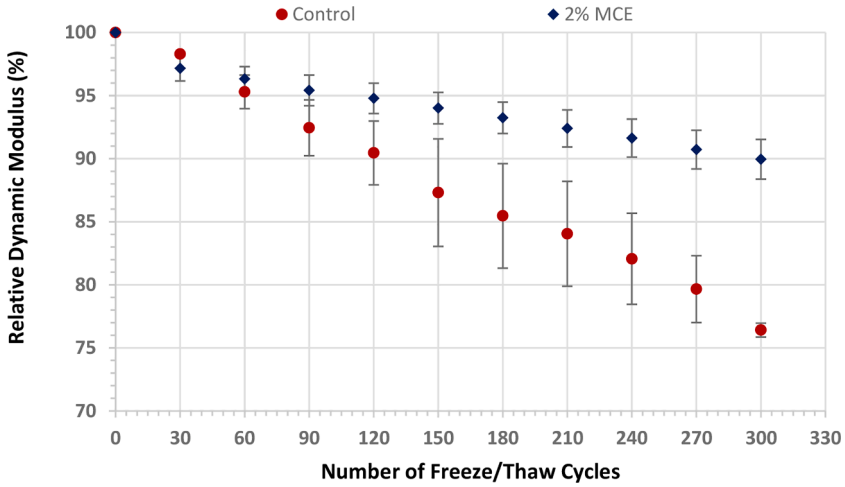

Fig. 9. curves of percentage relative dynamic modulus versus number of freezing and thawing cycles using modified ASTM C666 (i.e. cycling under more extreme temperatures of −53 to 22 °C) for control sample with concrete mixed with 2% MCE, (C4WRC20 at w/c of 0.40). The standard errors of three replicates are shown as error bars.

Table 7
percentage enhancement of concrete resistance against cycles of freezing and thawing for MCE-dosed after 300 cycles (comparing control sample with concrete mixed with 2% MCE, (C4WRC20 at w/c of 0.40).

Parameter (after 300 Cycles)	Percentage
reduction in the mass loss	92%
reduction in the percentage length change	15%

damages under cycles of freezing (investigating the icephobocity of MCE system is being performed in an ongoing research project).

3.5. Thermal and electrical resistivities

The aforementioned thermal performance of MCE is attributed to reducing the thermal conductivity (k) of concrete (increasing its the thermal resistance). Table 8 lists the average values of thermal conductivity and resistances against thermal and electrical conduction for concrete of C4WRC20 mix design at w/c ratio of 0.45 as averages of two replicated specimens. The obtained low thermal resistivity values for MCE-dosed concrete minimizes the rate of heat loss under freezing. The

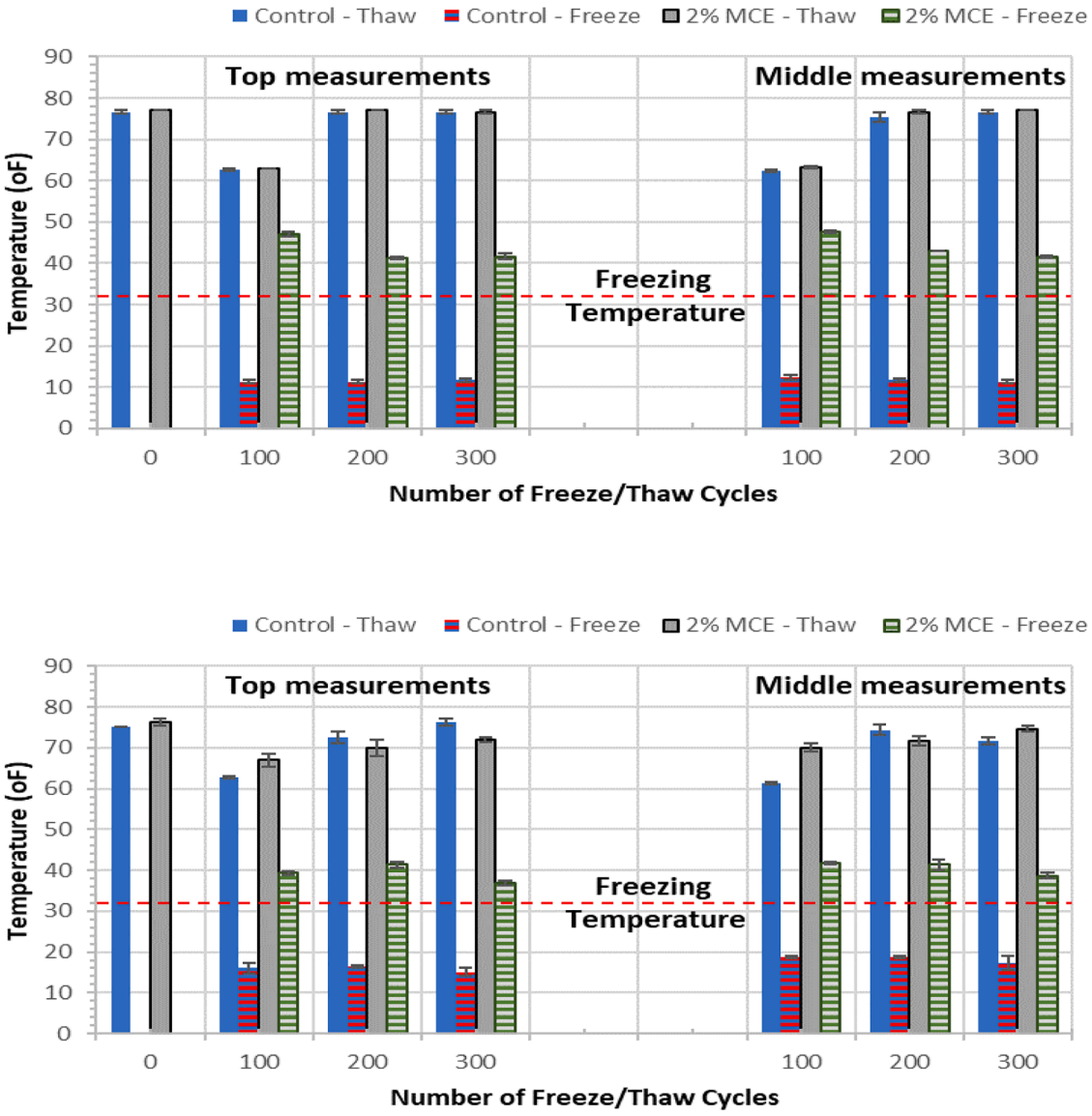

Fig. 10. concrete temperatures (at 1.27 cm depth below the surface) as functions of number of freezing and thawing cycles under the same conditions in Figs. 8 and 9. The standard errors of three replicates are shown as error bars.

Table 8
thermal conductivity and resistances against thermal and electrical conduction for concrete of C4WRC20 mix design.

Specimen	Thermal Conductivity (K) BTU/°F ft2 hr		Average Thermal Resistance (R) °F ft2 hr / BTU	Total Charge Passage (ASTM C-1202) Coulombs	rating (according to ASTM 1202)
Control Concrete	**1.92**	**1.96**	**0.52**	646	very low
MCE-dosed concrete	**1.61**	**1.67**	**0.62**	60	negligible
% Improvement	**16.1%**	**14.8%**	**19%**	**90.7%**	

enhancement of concrete mixtures with MCE increases the thermal resistivity of concrete by about 15–16%. This is also associated with a decrease in electrical conductivity as indicated by about 90% reduction the total charge passage as listed in Table 8. This increase in thermal resistivity (and the electrical resistivity) can be explained by the pore blocking mechanism of MCE and the reduction in internal moisture content as reported in a previous publication [29]. Hence, the decrease in thermal conductivity is associated with a decrease in the hydraulic and mass conductivities (or diffusivities) indicated as electrical conductivity (according to ASTM C-1202). The reduction in coefficient of permeability (according to the United States Corps of Engineering method specified in CRD-C 48–92 at a pressure of 1.4 MPa [51]) has been found to be more than 99% (results of unpublished research). The reductions in mass and hydraulic diffusivities are larger than those in thermal conductivity. In fact, the thermal diffusivity is also associated with the specific heat: this will be further investigated in an ongoing research project.

3.6. Summary of results and theoretical aspects

The role of MCE in managing thermal effects in concrete is achieved by its ability to control the rate of heat release during the initial cement hydration process and to shift the curve of cumulative heat release. This reduces the premature losses of moisture and hence enhance the mechanical characteristics of cured concrete. When applied to mass concrete, these thermal effects cause lowering the maximum temperature and decreasing the internal temperature gradients within mass concrete (since the addition of MCE causes shifts in the peak of maximum heat rate and in the curve of cumulative heat release). Hence, these effects lead to a more durable mass concrete. The ability of MCE to store the initial heat release for a longer period of time and its effect in lowering thermal conductivity promote its application for curing concrete under freezing conditions. These effects are associated with the ability of MCE to prevent freezing of water within concrete pores. This thermal ability for resisting freezing during curing under severe cold conditions is also associated with MCE ability to resist freezing and thawing cycles, as indicated in reductions in the percentage losses in dimensional stability (percentage mass change and percentage length change) as well as enhancement in the percentage relative dynamic modulus.

The theoretical analysis of MCE thermal performance can be summarized by the followings: (1) reducing the thermal conductivity as a result of reducing concrete porosity and permeability and moisture content, (2) managing phase change within concrete pores as the MCE crystals contribute with an additional phase change process through the adsorption/ desorption of water vapor by its hygroscopic crystal (which enhances the storage of thermal energy) (3) managing moisture content though combined heat and mass transfer processes associated with the aforementioned phase change processes (between moisture and crystals i.e. the reversible vapor storage within its hygroscopic crystals), (4) preventing freezing in fresh concrete through heat generation and storage which is associated with additional heat sources generated from the chemical reactions of the exothermic MCE crystallization process during concrete curing and its ability to reduce thermal conductivity and (5) minimizing ice adhesion due to lowering the water permeability of MCE-dosed concrete and consuming any available moisture through its dynamic crystal growth as well as its hydrophobicity which is theoretically corelated to icephobocity.

4. Conclusions and recommendations

Adding MCE to concrete mixtures is shown to effectively manage the thermal effects in concrete. The addition of MCE to the concrete mixture at dosage of 2% of cement weight can achieve the following thermal performances:

1) Delaying the exothermic heat release and reduces its rate at the initial stage.
2) Promoting the cement hydration reactions even under severe could conditions, when the concrete is allowed for an initial controlled curing for 24 h.
3) Increasing concrete resistance against cycles of freezing and thawing by reducing the percentage mass change (by 92%) and percentage length change (by 15%) and by increasing the relative dynamic modulus (by 17%) after 300 cycles.
4) Reducing the thermal conductivity by about 16% and reducing the total electrical charge passage by 90.7%.

The recommendations for further research work include

- In-depth investigation of mitigating the thermal effects using MCE in mass concrete.
- In-depth of investigation of the effect MCE dosage on thermal characteristics (thermal conductivity and specific heat).

Declaration of interests

The performance testing was performed by an independent material testing lab (testing certificates are available). There is no conflict of interest regarding the publication of this paper.

Acknowledgment(s)

The authors acknowledge the contribution of Dr. Xinbao Yu and Mr. Gang Lei, from the University of Texas at Arlington (UTA), Arlington, Texas, USA, for running the calorimetry test of cement hydration and providing the calorimetric data.

References

[1] M. Al-Jabari, 2 - Concrete porosity and transport processes, in: M. Al-Jabari (Ed.), Integral Waterproofing of Concrete Structures, Woodhead Publishing, 2022, pp. 37–68. Editor.
[2] M. Al-Jabari, 3 - Concrete durability problems: physicochemical and transport mechanisms, in: M. Al-Jabari (Ed.), Integral Waterproofing of Concrete Structures, Woodhead Publishing, 2022, pp. 69–107. Editor.
[3] S. Jianxia, 6.14 - Durability Design of Concrete Hydropower Structures, in: A. Sayigh (Ed.), Comprehensive Renewable Energy, Elsevier, Oxford, 2012, pp. 377–403. Editor.
[4] M. Al-Jabari, et al., 4 - Materials selection and proportioning for watertight and durable concrete, in: M. Al-Jabari (Ed.), Integral Waterproofing of Concrete Structures, Woodhead Publishing, 2022, pp. 109–134. Editor.
[5] P.K. Mehta, P.J. Monteiro, Concrete microstructure, Properties and Materials, McGraw-Hill Publishing, New York, NYUSA, 2017, 10019.
[6] K. Wang, et al., Permeability study of cracked concrete, Cement and concrete research 27 (3) (1997) 381.
[7] M. Al-Jabari, M. Husein, 5 - Physical and chemical interactions of water with surfaces and particles, in: M. Al-Jabari (Ed.), Integral Waterproofing of Concrete Structures, Woodhead Publishing, 2022, pp. 135–163. Editor.
[8] M. Al-Jabari, 1 - Introduction to concrete chemistry, in: M. Al-Jabari (Ed.), Integral Waterproofing of Concrete Structures, Woodhead Publishing, 2022, pp. 1–36. Editor.
[9] J.W. Bullard, et al., Mechanisms of cement hydration, Cement and concrete research 41 (12) (2011) 1208–1223.
[10] J.D. Bapat, Mineral Admixtures in Cement and Concrete, CRC Press, 2012.
[11] N. Mostafa, P. Brown, Heat of hydration of high reactive pozzolans in blended cements: isothermal conduction calorimetry, Thermochim Acta 435 (2) (2005) 162–167.
[12] E. Knapen, D. Van Gemert, Cement hydration and microstructure formation in the presence of water-soluble polymers, Cement and concrete Research 39 (1) (2009) 6–13.
[13] P. Livesey, A. Donnelly, C. Tomlinson, Measurement of the heat of hydration of cement, Cement and concrete composites 13 (3) (1991) 177–185.
[14] G. Artioli, J.W. Bullard, Cement hydration: the role of adsorption and crystal growth, Crystal Research and Technology 48 (10) (2013) 903–918.
[15] D. Marchon, R.J. Flatt, 8 - Mechanisms of cement hydration, in: P.-C. Aïtcin, R. J. Flatt (Eds.), Science and Technology of Concrete Admixtures, Woodhead Publishing, 2016, pp. 129–145.
[16] P. Mounanga, et al., Predicting Ca (OH) 2 content and chemical shrinkage of hydrating cement pastes using analytical approach, Cement and Concrete Research 34 (2) (2004) 255–265.

[17] G. Ye, Experimental Study and Numerical Simulation of the Development of the Microstructure and Permeability of Cementitious Materials, Delft University of Technology, TU Delft, The Netherlands, 2003.
[18] P.R. de Matos, et al., Effectiveness of fly ash in reducing the hydration heat release of mass concrete, Journal of Building Engineering 28 (2020), 101063.
[19] S. Han, Assessment of curing schemes for effectively controlling thermal behavior of mass concrete foundation at early ages, Construction and Building Materials 230 (2020), 117004.
[20] Y.-.Y. Chen, Effects Observed in Temperature Rise Evaluation Tests for Mass Concrete, 技術學刊 34 (2) (2019) 81–94.
[21] J. Gajda, M. Vangeem, Controlling temperatures in mass concrete, Concrete international 24 (1) (2002) 58–62.
[22] A.K. Saha, et al., The ASR mechanism of reactive aggregates in concrete and its mitigation by fly ash: a critical review, Construction and Building Materials 171 (2018) 743–758.
[23] H. Hamid, M.G. Chorzepa, Novel Structural Materials for Use in Mass Concrete Structures, in: Structures Congress 2019: Blast, Impact Loading, and Research and Education, American Society of Civil Engineers, Reston, VA, 2019.
[24] M. Al-Jabari, 6 - Fundamentals and categorizations of waterproofing technologies, in: M. Al-Jabari (Ed.), Integral Waterproofing of Concrete Structures, Woodhead Publishing, 2022, pp. 165–198. Editor.
[25] M. Al-Jabari, 7 - Concepts and types of integral waterproofing materials, in: M. Al-Jabari (Ed.), Integral Waterproofing of Concrete Structures, Woodhead Publishing, 2022, pp. 199–246. Editor.
[26] M. Al-Jabari, 9 - Hydrophilic crystallization waterproofing, in: M. Al-Jabari (Ed.), Integral Waterproofing of Concrete Structures, Woodhead Publishing, 2022, pp. 283–322. Editor.
[27] M. Al-Jabari, 8 - Hydrophobic integral dampproofing materials, in: M. Al-Jabari (Ed.), Integral Waterproofing of Concrete Structures, Woodhead Publishing, 2022, pp. 247–282. Editor.
[28] R. Al-Rashed, Multiple Crystallization Enhance (MCE) Intermix for Portland Cement Concrete, Google Patents, 2021.
[29] R. Al-Rashed, M. Al-Jabari, Multi-crystallization enhancer for concrete waterproofing by pore blocking, Construction and Building Materials 272 (2021), 121668.
[30] R.D. Mundo, et al., Recent Advances in Hydrophobic and Icephobic Surface Treatments of Concrete, Coatings 10 (5) (2020) 449.
[31] P. Azarsa, R. Gupta, A. Biparva, Assessment of self-healing and durability parameters of concretes incorporating crystalline admixtures and Portland Limestone Cement, Cement and Concrete Composites 99 (2019) 17–31.
[32] K.S. Appelbaum, J.T. Stewart, G.R. Hartwell, Effect of sodium fluorosilicate on the properties of Portland cement, J Endod 38 (7) (2012) 1001–1003.
[33] R. Al-Rashed, M. Jabari, Dual-crystallization waterproofing technology for topical treatment of concrete, Case Studies in Construction Materials 13 (2020) e00408.
[34] R. Al-Rashed, M. Al-Jabari, Concrete Protection by Combined Hygroscopic and Hydrophilic Crystallization Waterproofing Applied to Fresh Concrete, Case Studies in Construction Materials 15 (2021) e00635.
[35] A.A. Almusallam, et al., Effectiveness of surface coatings in improving concrete durability, Cement and Concrete Composites 25 (4) (2003) 473–481.
[36] X. Pan, et al., A review on surface treatment for concrete – Part 2: performance, Construction and Building Materials 133 (2017) 81–90.
[37] X. Pan, et al., A review on concrete surface treatment Part I: types and mechanisms, Construction and Building Materials 132 (2017) 578–590.
[38] N.Z. Muhammad, et al., Waterproof performance of concrete: a critical review on implemented approaches, Construction and Building Materials 101 (2015) 80–90.
[39] M.L. Berndt, Evaluation of coatings, mortars and mix design for protection of concrete against sulphur oxidising bacteria, Construction and Building Materials 25 (10) (2011) 3893–3902.
[40] P. Azarsa, R. Gupta, A. Biparva, Inventive Microstructural and Durability Investigation of Cementitious Composites Involving Crystalline Waterproofing Admixtures and Portland Limestone Cement, Materials (Basel) 13 (6) (2020) 1425.
[41] A. de Souza Oliveira, et al., Crystalline admixture effects on crystal formation phenomena during cement pastes' hydration, J Therm Anal Calorim 139 (6) (2020) 3361–3375.
[42] P. Reiterman, et al., Reduction of concrete surface permeability by using crystalline treatment, Revista Romana de Materiale 50 (1) (2020) 69–74.
[43] H. Žáková, J. Pazderka, P. Reiterman, Textile Reinforced Concrete in Combination with Improved Self-Healing Ability Caused by Crystalline Admixture, Materials (Basel) 13 (24) (2020) 5787.
[44] Iowa-DOT, Portland Cement (PC) Concrete Proportions, Iowa Department of Transportation, Iowa, USA, 2014.
[45] ASTM, C666 /C666M - 15, Standard Test Method for Resistance of Concrete to Rapid Freezing and Thawing. Annual Book of ASTM Standards, ASTM International, West Conshohocken, PA, USA, 2015.
[46] ASTM, C168, Standard Terminology Relating to Thermal Insulation. Annual Book of ASTM Standards, ASTM International, West Conshohocken, PA, USA, 2005.
[47] A. Biparva, R. Gupta, Smart Waterproofing System: a Review, in: Proceedings of the International Conference on Future Concrete, 2010.
[48] J. Pazderka, E. Hájková, Crystalline admixtures and their effect on selected properties of concrete, Acta Polytechnica 56 (4) (2016) 306–311.
[49] K. Gyu-Yong, et al., Evaluation of properties of concrete using fluosilicate salts and metal (Ni, W) compounds, Transactions of Nonferrous Metals Society of China 19 (2009) s134–s142.
[50] W.-.C. Choi, B.-.S. Khil, H.-.D. Yun, Characteristics of structural concrete containing fluorosilicate-based admixture (FBA) for improving water-tightness, Construction and Building Materials 74 (2015) 241–248.
[51] CRD, C48-92 Standard Test Method for Water Permeability of Concrete, U.S. Army Corps of Engineers, 1992.